Transactions of the SMiRT 27
Yokohama, Japan, March 3-8, 2024
Division V

BI-DIRECTIONAL CHARACTERIZATION TEST OF A FRICTION PENDULUM BEARING WITH REAL-TIME AXIAL FORCE CONTROL

Chunghyun Lee[1], Yunbyeong Chae[2]

[1] Master Student, Seoul National University, Seoul, Republic of Korea (aniori37@snu.ac.kr)
[2] Associate Professor, Seoul National University, Seoul, Republic of Korea (ybchae@snu.ac.kr)

ABSTRACT

It is important to precisely control the axial force during characterization tests for a friction pendulum (FP) bearing since the frictional behavior of the FP bearing is highly dependent on the axial pressure and sliding velocity. However, it is difficult to control the axial force because of the vertical motion induced by the spherical sliding surface of the FP bearing, where the force control is highly sensitive to the vertical motion. This study aims to conduct a characterization test for a single concave FP bearing with the use of advanced force control method. Through a series of dynamic tests, the axial force control performance will be evaluated, and the frictional behavior of the FP bearing will be characterized under various constant axial pressures and sliding velocities. The whole tests will be performed in January 2024, and the test results will be shared in the conference.

INTRODUCTION

Friction pendulum (FP) bearings, also referred to as friction pendulum systems (FPS), have been used in a range of structural systems which require seismic isolation, including critical facilities such as nuclear power plants (Kim, 2009). FP bearings offer effective seismic protection through their energy dissipating ability via sliding friction mechanisms. It is important to reliably identify the frictional characteristics of the FP bearing because its behavior is highly dependent on the frictional force between the concave surface and the slider.

There have been several experimental studies that tried to identify the frictional characteristics of friction-based seismic isolation devices. Mokha et al. (1990) and Constantinou et al. (1990) evaluated frictional characteristics of polytetrafluorethylene (PTFE)-stainless steel surface through experiments on plane PTFE interfaces to model the behavior of Teflon sliding bearings, and they concluded that bearing pressure and sliding velocity have a significant effect on the coefficient of friction. Constantinou et al. (1999) performed an experiment on the sliding interface of a PTFE-stainless steel sliding bearing and verified how much the environmental factors such as pressure, temperature, and sliding velocity influences the frictional behavior. Mosqueda et al. (2004) conducted characterization test on single FP bearings with various bi-directional orbits and earthquake ground motions and confirmed that coefficient of friction is affected by bearing pressure, sliding velocity, and frictional heating. Kumar et al. (2015) analysed experimental data of previous studies and built numerical model for single concave FP bearings, which includes factors related to axial pressure, sliding velocity and temperature at the sliding surface. Furinghetti et al. (2019) implemented a cyclic response test on a double concave FP bearing, and assessed the effect of axial pressure, sliding speed and abrasion due to sustained motion. Although each of studies slightly differs in methods of experiments and modeling of frictional behavior, all of them pointed out that coefficient of friction on the sliding surface is highly dependent of axial pressure and sliding velocity. Therefore, it can be said that precise control of axial pressure and sliding velocity during an experiment is essential for the accurate evaluation of the frictional behavior of FP bearings.

However, it is challenging to constantly maintain the desired axial pressure applied to the FP bearing during the lateral motion of the bearing, due to geometric characteristics of spherical sliding surface and the sensitivity of axial force control on the change of vertical displacement. While an FP bearing travels along horizontal orbits, the mass on the FP bearing moves up and down in accordance with the curvature

of the sliding surface and the vertical motion makes it difficult to control the axial force acting on the FP bearing. If a certain mass is installed over the FP bearing instead of controlling the axial load with actuators, the vertical inertia force of the mass is relatively small compared to the weight, thus a constant axial force can be maintained during the lateral motion of the bearing; however, the test setup becomes massive, and, most importantly, it is difficult to modify the axial pressure applied to the FP bearing as desired.

The aim of this study is to carry on a characterization test for a small-scale single FP bearing with well-controlled axial pressure, which can be achieved with the advanced real-time force control method originally developed by Chae et al. (2019) and further improved by Cho et al. (2023). Using a test setup with three horizontal actuators and one vertical actuator connected with a flexible loading frame (FLF), it becomes possible to consistently apply bi-directional lateral displacements and time-varying (or constant) axial forces to the bearing. This configuration allows for the reliable testing of several uni-directional and bi-directional orbits on the FP bearing. The tests will vary axial pressure and sliding velocities to comprehensively characterize the frictional behavior of the FP bearing. Additionally, an analytical model for the FP bearing will be developed based on the experimental data. The entire test program is scheduled to be conducted in January 2024.

MODIFIED D-ATS FORCE CONTROL METHOD

Chae et al. (2013) introduced the adaptive time series (ATS) compensator which significantly improved real-time displacement control for servo-hydraulic actuators. Chae et al. (2017) developed the D-ATS force control method, which uses the ATS compensator with a compliance spring that converts a force control problem into a displacement control problem. The ATS compensator minimizes the phase and amplitude errors by providing a compensated input to the actuator. The compensated input displacement u_c is calculated as:

$$u_c = a_0 x_t + a_1 \dot{x}_t + a_2 \ddot{x}_t \tag{1}$$

where, x_t, $\dot{x}_t$, and $\ddot{x}_t$ are the target displacement, target velocity, and target acceleration of the actuator, respectively. a_0, a_1, and a_2 are the system coefficients which are updated at each time step in a way to minimize the error between the target and measured displacements. The compliance spring is designed to remain linear-elastic within the range of force applied during the experiments, therefore the target displacement of the actuator x_t is determined as follows:

$$x_t = f_t/k_c + x_s \tag{2}$$

where f_t, k_c, and x_s are the target force, the stiffness of the compliance spring, and the displacement of test specimen, respectively. Substituting Equation (2) into Equation (1), the compensated input displacement can be expressed as:

$$u_c = a_0\left(\frac{f_t}{k_c} + x_s\right) + a_1\left(\frac{\dot{f}_t}{k_c} + \dot{x}_s\right) + a_2\left(\frac{\ddot{f}_t}{k_c} + \ddot{x}_s\right) \tag{3}$$

Chae et al. (2018) installed additional sensors to the specimen to acquire the current state of the specimen, x_s, $\dot{x}_s$, and $\ddot{x}_s$. Cho et al. (2023) improved the D-ATS method to obtain the displacement of the test specimen through indirect way so that no additional sensors are needed. The deformation in the compliance spring is in proportion with the force applied with the actuator, and the displacement of the actuator is identical to the sum of deformation in the compliance spring and the test specimen, thus x_s of Equation (3) can be estimated as follow:

$$x_s = x_a - f_a/k_c \tag{4}$$

where x_a and f_a are the actuator displacement and force measured by the sensors embedded in the actuator. Then, $\dot{x}_s$ and $\ddot{x}_s$ can be calculated through numerical differentiation of x_s. Substituting Equation (4) to (3), the input actuator displacement for the modified D-ATS force control method is given as follows:

$$u_c = a_0\left(\frac{f_t - f_a}{k_c} + x_a\right) + a_1\left(\frac{\dot{f}_t - \dot{f}_a}{k_c} + \dot{x}_a\right) + a_2\left(\frac{\ddot{f}_t - \ddot{f}_a}{k_c} + \ddot{x}_a\right) \tag{5}$$

As the compensated input displacement u_c is put into the actuator, the actuator tracks the target force by controlling the displacement applied to the compliance spring. It has to be noted that the measured displacement and force of actuator in Equation (4) are noisy, thus the measured data of actuator must be filtered appropriately before substituted into Equation (4). Cho et al. (2023) used a polynomial regression-based (PR) state estimator to filter the noise in the measured signal. The study also introduced saturation process for the velocity of compensated input signal so that the oil-column resonance in the system can be effectively suppressed.

Chae et al. (2019) showed that the D-ATS force control method can be extended to a large axial force application case using a flexible loading beam (FLB) which is designed to exhibit a linear-elastic relationship between the force applied to the FLB and its flexural deformation. In this study, a flexible loading frame (FLF), which is a simple portal frame designed to bend linearly in proportion to the force applied, is used to implement the modified D-ATS force control method.

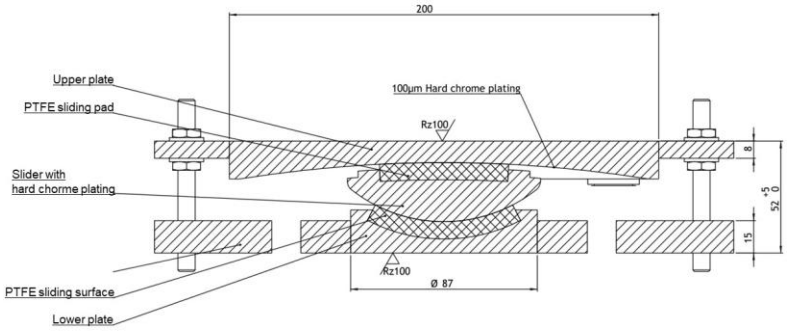

Figure 1. Cross section of the FP bearing.

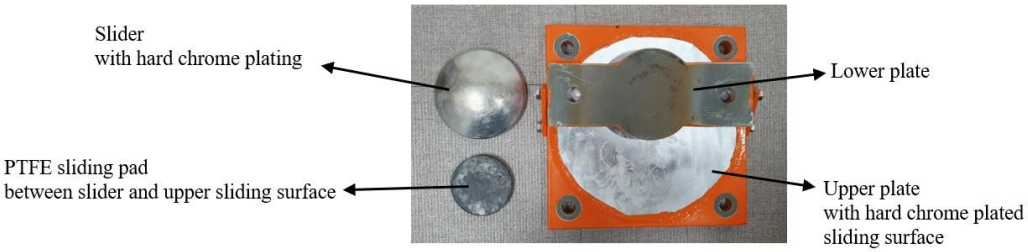

Figure 2. Components of the FP bearing.

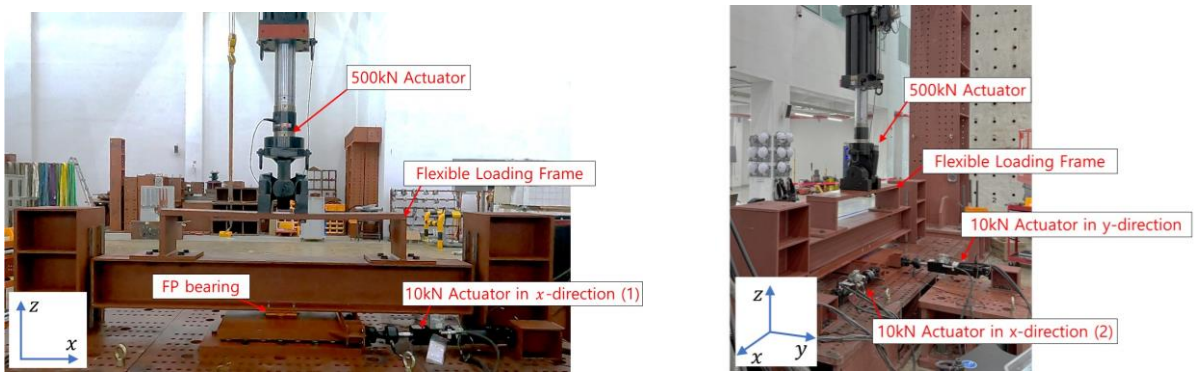

(a) Front view (b) Isometric rear view

Figure 3. Experimental test setup.

EXPERIMENTAL TEST SETUP

FP Bearing Test Specimen

The test specimen utilized in this study is a customized small-scale single concave FP bearing. The detailed cross section and overall components of the bearing are depicted in Figure 1 and 2, respectively. The downsizing of the prototype was necessitated by the limitations imposed by the load and displacement capacities of the actuators . The upper plate of the bearing is a square shape with 200mm each side and has a concave sliding surface. The sliding surface has an effective radius of curvature of R = 642.5 mm and has a design displacement range of 50 mm. The sliding surface is composed of stainless steel material and hard chrome-plate with an average surface roughness of 100 μm. Positioned between the upper plate and the slider is a slider pad composed of a PTFE-based compound. The slider, crafted from stainless steel, is also coated with hard chromium. The lower plate has a fixed PTFE sliding pad so that the slider only shows a rotational motion relative to the lower plate. The maximum design axial load capacity of the bearing is 100 kN.

Experimental Test Setup

Figure 3 depicts the experimental test setup established at the Extreme Performance Test Center of Seoul National University. The FP bearing is affixed to a square table supported by ball transfer bearings, facilitating horizontal movement in both directions. This square table is linked to three dynamic actuators, with two operating in the x-direction and one in the y-direction, enabling the imposition of various bi-directional displacements on the test specimen in real-time. Vertically, a 500 kN dynamic actuator is connected to the linear-elastic foundation (FLF) designed to withstand a maximum axial force of 100 kN. An H-beam is interposed between the FLF and the FP bearing, serving to transmit the vertical force from the FLF to the FP bearing. The H-beam is supported at both ends by guide rails, allowing only vertical movement without any rotation.

EXPERIMENTAL TESTING PLAN

All characterization tests are expected to be completely by January 2024, thus detailed test results and analysis will be provided and presented at the conference. This section describes the experiment program currently planned.

Evaluating Axial Force Control Performance

As mentioned in Introduction, there is vertical inertia force even if an FP bearing only subjected to horizontal displacements. Figure 4 shows the analytical vertical displacements when the test specimen moves along an uni-directional triangular wave with smoothed peak and a bi-directional cloverleaf orbit. When the peak displacement in horizontal direction is 45 mm, the peak vertical displacement of the test specimen is about 1.6 mm, which can cause significant impact to the vertical force control. Because of this vertical motion associated with the lateral movement of the FP bearing, the axial force control has been a challenging task in the existing studies, making it difficult to directly evaluate the lateral response of the FP bearing under constant axial forces.

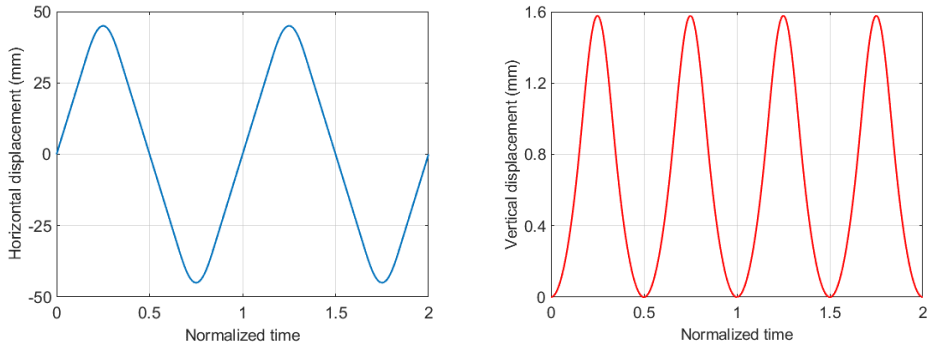

(a) uni-directional triangular wave with smoothed peak

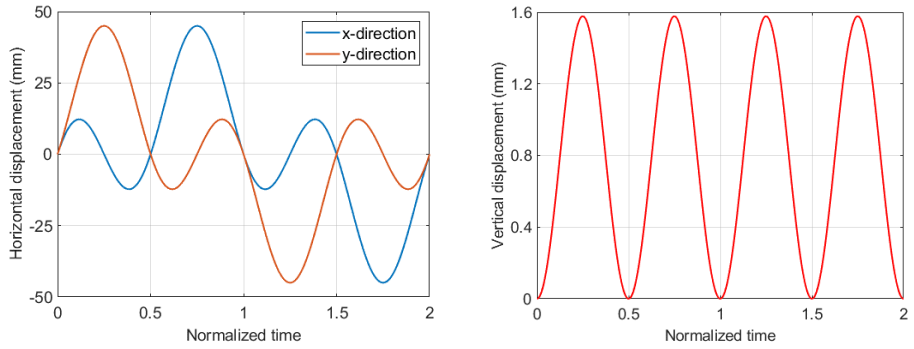

(b) bi-directional cloverleaf orbit

Figure 4. Horizontal and vertical displacements of test specimen for different orbits

Table 1: Tables should be centred and preceded by a numbered caption.

Case	Control method
1	PID controller without FLF (existing force control method)
2	PID controller with FLF
3	Modified D-ATS compensator with FLF

This study will try 3 cases of force control method as listed in Table 1. For each case, uni-directional and bi-directional orbits of Figure 4 will be used under different axial forces and sliding velocities, where the error between the target force and the measured force will be evaluated using the normalized root mean square (NRMS) error as follows:

$$\text{NRMS force error} = \sqrt{\frac{\sum_{i=1}^{N}\left(f_t^i - f_a^i\right)^2}{\sum_{i=1}^{N}\left(f_t^i\right)^2}} \tag{6}$$

In Equation (6), f_t^i and f_a^i are the target axial force and the measured axial force at the i-th time step, respectively, and N is the number of data points. It can be said that the method with the smaller NRMS force error has the better force control performance overall.

Characterization Test and Modeling of FP Bearing

The characterization test will be performed by applying various uni-directional and bi-directional horizontal motions while keeping the axial pressure and sliding velocity constant. The same orbits will be tested repeatedly with different axial pressures and velocities. To maintain the constant velocity during the test, a triangular wave will be used as uni-directional orbit instead of sinusoidal orbit. The sharp change of velocity at the peak of triangular wave will be smoothed using the polynomial curve fitting of velocity as shown in Figure 4(a). For bi-directional orbits, to maintain constant tangent velocity during the test, a resampling procedure introduced in Pavase (2018) will be applied to the horizontal displacement input. The effects of axial pressure, sliding velocity, path dependency, and wearing of slider on the lateral response will be investigated.

The frictional behavior of the FP bearing will be numerically modelled as a function of axial pressure, sliding velocity, and dissipated energy. Although many preceding studies have pointed out the temperature at the sliding surface as a major variable contributing to the frictional behavior, this study will adopt the dissipated energy as a modeling variable as Furinghetti (2019) proposed because of the difficulties in measuring the temperature at sliding surface. Furthermore, since the frictional heating is generally modelled as a function of contact pressure and sliding velocity (Amiri and Khonsari, 2010), the temperature rise by frictional heating can be indirectly included as a model of axial pressure, sliding velocity, and dissipated energy.

CONCLUDING REMARKS

Controlling the axial pressure applied to the FP bearing during characterization test is important because the frictional behavior of the FP bearing is highly dependent on the axial pressure. This study uses a recently developed real-time force control method with the use of FLF to achieve a stable control of the axial force during characterization test, which was difficult to achieve in the past. The performance of the modified D-ATS force control method will be compared with existing methods and validated by conducting uni- and bi-directional lateral displacement tests under various axial forces and velocities. The whole tests are expected to be completed by January 2024, and the test results as well as new findings will be shared in the conference.

ACKOWLEDGEMENTS

This study was supported by the National Research Foundation of Korea (NRF), a grant funded by the Ministry of Science and ICT (Grant No. 2022R1A2C2012494). The Extreme Performance Test Center at

Seoul National University provided test equipment and extensive support for the experimental program of this study. The authors express their sincere gratitude for their generous support.

NOMENCLATURE

a_0 : system coefficient for target displacement, identified to minimize the tracking error of the actuator
a_1 : system coefficient for target velocity, identified to minimize the tracking error of the actuator
a_2 : system coefficient for target acceleration, identified to minimize the tracking error of the actuator
f_a : measured force of actuator
f_a^i : measured force of actuator at i-th time step
f_t : target force of actuator
f_t^i : target force of actuator at i-th time step
k_c : stiffness of compliance spring
N : number of data points
u_c : compensated displacement input for actuator
x_a : measured actuator displacement
x_s : displacement of test specimen
x_t : target displacement of actuator

REFERENCES

Amiri, M., and Khonsari, M. M. (2010). "On the thermodynamics of friction and wear—a review." *Entropy*, 12(5), 1021-1049.

Chae, Y., Kazemibidokhti, K., Ricles, J.M. (2013) "Adaptive time series compensator for delay compensation of servo-hydraulic actuator systems for real-time hybrid simulation." *Earthquake Engineering and Structural Dynamics*, 42(11), 1697-1715.

Chae, Y., Rabiee, R., Dursun, A., Kim, C.Y. (2018). "Real-time force control for servo-hydraulic actuator systems using adaptive time series compensator and compliance springs." *Earthquake Engineering & Structural Dynamics*, 47(4), 854-871.

Chae, Y., Lee, J., Park, M., Kim, C.Y. (2019). "Fast and slow cyclic tests for reinforced concrete columns with an improved axial force control." *Journal of Structural Engineering*, 145(6), 04019044.

Cho, C.B., Chae Y., Park M. (2023). "Improved Real-Time Force Control for Applying Axial Force to Axially Stiff Members." *Earthquake Engineering & Structural Dynamics*, https://doi.org/10.1002/eqe.4024

Constantinou, M., Mokha, A., Reinhorn, A. (1990). "Teflon bearings in base isolation II: Modeling." *Journal of Structural Engineering*, 116(2), 455-474.

Constantinou, M.C., Tsopelas, P., Kasalanati, A., Wolff, E.D. (1999). "Property modification factors for seismic isolation bearings." *Technical Rep. MCEER-99-0012*, Multidisciplinary Center for Earthquake Engineering Research, Univ. at Buffalo, Buffalo, NY.

Furinghetti, M., Pavese A., Quaglini V., Dubini P. (2019). "Experimental investigation of the cyclic response of double curved surface sliders subjected to radial and bidirectional sliding motions." *Soil Dynamics and Earthquake Engineering*, 117, 190-202.

Kim, W. B., Lee, K., & Kim, G. H. (2009). "Application of friction pendulum system to the main control room of a nuclear power plant." *Canadian Journal of Civil Engineering*, 36(1), 63-72.

Kumar, M., Whittaker, A.S., Constantinou, M.C. (2015). "Characterizing friction in sliding isolation bearings." *Earthquake Engineering & Structural Dynamics*, 44(9), 1409-1425.

Mokha, A., Constantinou, M., Reinhorn, A. (1990). "Teflon bearings in base isolation I: Testing." *Journal of Structural Engineering*, 116(2), 438-454.

Mosqueda, G., Whittaker, A.S., Fenves, G.L. (2004). "Characterization and modeling of friction pendulum bearings subjected to multiple components of excitation." *Journal of Structural Engineering*, 130(3), 433-442.

Pavese, A., Furinghetti, M., & Casarotti, C. (2018). “Experimental assessment of the cyclic response of friction-based isolators under bidirectional motions.” *Soil Dynamics and Earthquake Engineering*, 114, 1-11.